Synchrotron Radiation from Electron Beams in Plasma Focusing Channels

E. Esarey, B.A. Shadwick, P. Catravas, and W.P. Leemans

Center for Beam Physics, Ernest Orlando Lawrence Berkeley National Laboratory, University of California, Berkeley CA 94720

(December 6, 2001)

Abstract

Spontaneous radiation emitted from relativistic electrons undergoing betatron motion in a plasma focusing channel is analyzed and applications to plasma wakefield accelerator experiments and to the ion channel laser (ICL) are discussed. Important similarities and differences between a free electron laser (FEL) and an ICL are delineated. It is shown that the frequency of spontaneous radiation is a strong function of the betatron strength parameter a_β, which plays a similar role to that of the wiggler strength parameter in a conventional FEL. For $a_\beta \gtrsim 1$, radiation is emitted in numerous harmonics. Furthermore, a_β is proportional to the amplitude of the betatron orbit, which varies for every electron in the beam. The radiation spectrum emitted from an electron beam is calculated by averaging the single electron spectrum over the electron distribution. This leads to a frequency broadening of the radiation spectrum, which places serious limits on the possibility of realizing an ICL.

03.65.-w, 02.60.Cb, 32.80.-t, 02.70.-c

I. INTRODUCTION

The propagation of electrons beams through plasmas is relevant to a variety of advanced accelerators [1] - [5] and novel radiation sources, such as the plasma-focused free electron laser (FEL) [6] - [10], the plasma-wiggler FEL [11], [12], the ion-ripple laser [13], and the ion-channel laser [14]. Recent experiments that explore the interaction of an intense electron bunch with a plasma include the plasma wakefield accelerator (PWFA) experiment at Argonne National Laboratory [3], the E-150 plasma lens experiment at Stanford Linear Accelerator Center (SLAC) [4], and the E-157 PWFA experiment at SLAC [5]. In the E-157 experiments, a 30 GeV electron beam of 2×10^{10} electrons in a 0.65 mm long bunch is propagated through a 1.4 m long lithium plasma with an electron density up to 2×10^{14} cm^{-3}. The electron bunch propagates through the plasma in the so-called blowout regime [15], i.e., the initial beam density is greater than the plasma density. In this regime, the head of the bunch expels the plasma electrons and leaves behind a nearly uniform ion channel. The bunch length and plasma density are chosen such that the blown-out plasma electrons come crashing back to the axis near the tail of the bunch, thus driving a very large axial electric field, on the order of several hundred MV/m, that can accelerate the electrons in the tail of the bunch. The blow-out regime of the PWFA can be viewed as a short-bunch version of the ion-focused regime of electron beam propagation [16] - [19]. The "ion-focused regime" is a phrase traditionally applied to describe the propagation of long (compared to the plasma wavelength) electron beams in a plasma and, hence, these beams are subject to the electron-hose instability [20] - [23].

One consequence of operating in the blowout regime of the PWFA is that the main body of the electron bunch resides in the nearly uniform ion channel, since the plasma electrons are blown out to approximately the plasma skin depth, $k_p^{-1} = c/\omega_p$, which is typically much greater than the bunch radius, where $\omega_p = (4\pi n_e e^2/m_e)^{1/2}$ is the plasma frequency and n_e is the electron plasma density. Associated with the ion channel are very strong transverse fields, on the order of several thousand Tesla per meter, that subsequently focus the body

of the electron bunch. Since the initial beam radius ($50 - 100$ μm) is much greater than the matched beam radius (~ 5 μm), the beam radius will undergo betatron oscillations as it propagates through the plasma [5], [14]. In the blowout regime, the radial space charge electric field [5] is $E_r = (em_e/c^2)k_p^2 r/2$. At the edge of the beam, $r = r_b$, this can be written in convenient units as

$$E_r[\mathrm{MV/m}] = 9.06 \times 10^{-15} n_e[\mathrm{cm}^{-3}] r_b[\mu\mathrm{m}]. \tag{1}$$

Likewise, in the blowout regime, the betatron wavelength is $\lambda_\beta = (2\gamma)^{1/2}\lambda_p$, where γ is the relativistic factor of the electron and $\lambda_p = 2\pi/k_p$ is the plasma wavelength, which can be written as

$$\lambda_p[\mathrm{cm}] = 3.34 \times 10^6 (n_e[\mathrm{cm}^{-3}])^{-1/2}. \tag{2}$$

Time-integrated optical transition radiation has been used to study the transverse beam profile dynamics in the E-157 experiments [24], [25], where up to three betatron oscillations of the beam radius have been observed [25], [26].

In addition to the blowout regime of the PWFA, an accelerated electron bunch will experience transverse focusing forces in typical plasma-based accelerators, such as the laser wakefield accelerator (LWFA) [1]. For example, in the linear regime of the LWFA, the wakefield is often described by an electrostatic potential of the form $\Phi = \Phi_0 \exp(-r^2/r_p^2)\cos k_p(z - ct)$, where r_p is the radius of the wake and is proportional to radius of the drive beam. Notice that the axial electric field $E_z = -\partial\Phi/\partial z$ and the radial electric field $E_r = -\partial\Phi/\partial r$ are phased such that there exists a $\pi/2$ region of axial phase $k_p(z - ct)$ that is both accelerating and focusing. An electron residing off-axis will undergo radial betatron oscillations about the axis due to the transverse focusing force of the wakefield. The magnitude of the focusing field near the axis is $|E_r| \simeq 2r\Phi_0/r_p^2$, assuming $\cos k_p(z - ct) \simeq 1$, and the betatron wavelength is $\lambda_\beta = \pi r_p(2\gamma/\hat{\Phi}_0)^{1/2}$, where $\hat{\Phi}_0 = e\Phi_0/m_e c^2$ is the normalized amplitude of the wakefield. The density perturbation on axis associated with the wake is given by $\delta n_e/n_e = -\hat{\Phi}_0(1 + 4/k_p^2 r_p^2)\cos k_p(z - ct)$. Electron blowout near the axis occurs when $\hat{\Phi}_0 \simeq k_p^2 r_p^2/4$, assuming $k_p r_p/2 < 1$.

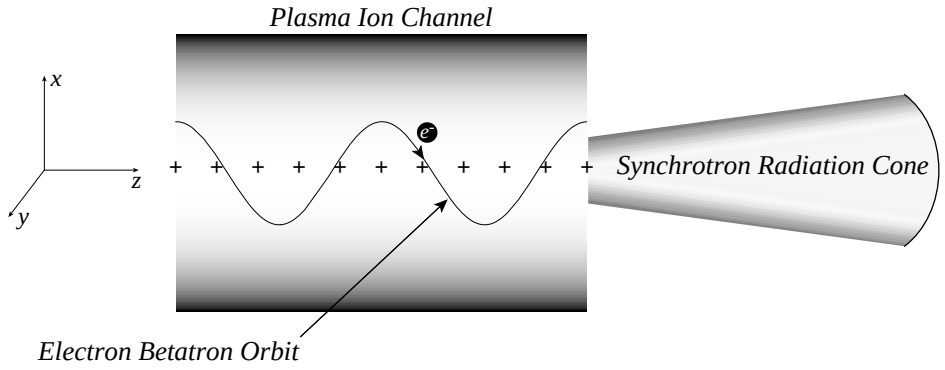

FIG. 1. Schematic of an electron undergoing betatron oscillations in a plasma focusing channel and emitting synchrotron radiation.

As an electron undergoes betatron oscillations in a plasma focusing channel, it will emit synchrotron radiation [14], [27], [28] (see Fig. 1). In the limit of a small amplitude betatron orbit, i.e., an electron displaced slightly from the axis, the wavelength of the synchrotron radiation is $\lambda = \lambda_\beta/2\gamma^2$. For plasma-based accelerators, this can easily be in the hard X-ray range, e.g., in the E-157 experiment, $\lambda_\beta \sim 0.8$ m and $\gamma = 6 \times 10^4$, such that $\lambda \sim 0.1$ nm. Preliminary observations of X-rays generated by this mechanism at 6.4 keV have been reported in the E-157 experiments [29].

The betatron motion in a focusing channel also forms the basis of the ion channel laser (ICL) [14]. In the ICL, radiation at the resonant wavelength $\lambda = \lambda_\beta/2\gamma^2$ can feed back on the electron beam, leading to axial bunching of the beam, and coherent amplification of the radiation. The amplification process is analogous to that in a free electron laser (FEL), with the betatron motion analogous to the electron motion in an FEL wiggler [30]. It has been suggested that the ICL mechanism can further enhance the spontaneous synchrotron radiation in the E-157 experiments [31], thus leading to partially coherent radiation near 0.1 nm. It is necessary that the details of the single particle synchrotron radiation in a plasma focusing channel be well understood, in order to assess the prospects for the generation of self-amplified spontaneous emission (SASE) in an ICL.

The ICL differs from other FEL concepts in that no external magnets, cavities, or slow wave structures are required for amplification. In particular, the ICL differs fundamentally

from the plasma-focused FEL [6] - [10], in which the FEL interaction is based on the wiggler magnet (with period λ_w) and radiation is emitted at the resonant wavelength $\lambda = \lambda_w/2\gamma^2$. In the conventional plasma-focused FEL, the plasma acts primarily to provide transverse focusing of the electron beam and the plasma density is sufficiently low such that $\lambda_\beta \gg \lambda_w$. The advantage of the ICL is that a wiggler magnet is no longer required, since the plasma serves to both focus the electron beam and to provide a resonant interaction for radiation of wavelength $\lambda = \lambda_\beta/2\gamma^2$.

Experiments on the ICL have been carried out by Whittum et al. [32] in the microwave regime. These experiments used a 0.75 MeV, 100 ns, 3.4 kA electron beam propagating through a plasma of density 4×10^{10} cm^{-3} ($\lambda_\beta \simeq 40$ cm) at a channeled radius of 1 cm. Input radiation at 9.4 GHz was amplified from 20 kW to several hundred kW after propagating 2.8 m through the plasma. In these experiments, the betatron strength parameter (discussed below) was $a_\beta < 0.5$.

In this article, spontaneous radiation emitted from an electron undergoing betatron motion in a plasma focusing channel is analyzed starting from basic principles. Application of these results to the E-157 experiment and to the ICL are examined. Important similarities and differences between SASE in an FEL and in an ICL are delineated. It is shown that the spontaneous radiation emitted along the axis of a plasma focusing channel from a single electron occurs near the resonant frequency $\omega_n = 2\gamma_{z0}^2 n\omega_\beta/(1 + a_\beta^2/2)^{1/2}$, where γ_{z0} is the relativstic factor for the electron entering the channel, n is the harmonic number, $\omega_\beta = ck_\beta = 2\pi c/\lambda_\beta$ is the betatron frequency, $a_\beta = \gamma_{z0} k_\beta r_\beta$ is the betatron strength parameter, and r_β is the amplitude of the betatron orbit. The role of the betatron strength parameter a_β is analogous to that of the wiggler strength parameter a_w (or K_w) in FEL physics. In Ref. [14], the ICL was considered only in the limit $a_\beta^2 \ll 1$. When $a_\beta^2 \ll 1$, radiation is emitted primarily at the fundamental frequency $\omega = 2\gamma_{z0}^2\omega_\beta$ and is independent of a_β. For $a_\beta \gtrsim 1$, however, radiation is emitted in numerous harmonics and the resonant frequency is a strong function of a_β. This is the case in the E-157 experiments, where $a_\beta \sim 2 - 50$. In an ideal FEL, the wiggler strength parameter a_w is a constant (a function

of only the magnetic field of the wiggler) for all of the beam electrons. However, in an ICL, $a_\beta = \gamma_{z0} k_\beta r_\beta$ depends on both the electron energy γ_{z0} and the betatron amplitude r_β. Since r_β, and hence a_β, is different for every electron in a typical beam, this places serious limits on the possibility of realizing a SASE ICL.

The remainder of this article is organized as follows. Section II discusses the motion of a single electron, as well as of the radius of an electron beam, in a plasma focusing channel. In Sec. III, the synchrotron radiation from a single electron in a plasma focusing channel is analyzed, including derivations of the general radiation spectrum for arbitrary a_β, as well as asymptotic expressions valid in the $a_\beta^2 \gg 1$ limit. Section IV discusses the total power radiated and the electron energy loss. In Sec. V, the radiation spectrum from a round (axisymmetric) electron beam is analyzed, as obtained by averaging the single electron spectrum over a Gaussian radial beam profile. Section VI discusses applications to the ion channel laser. A summary discussion is presented in Sec. VII.

II. ELECTRON MOTION IN PLASMA FOCUSING CHANNELS

A. Single Particle Orbits

The electron motion in a plasma focusing channel is governed by the relativistic Lorentz equation, which may be written in the form

$$d\mathbf{u}/dct = \nabla\hat{\Phi} \tag{3}$$

where $\hat{\Phi} = e\Phi/m_e c^2$ is the normalized electrostatic potential of the focusing channel, $\mathbf{u} = \mathbf{p}/m_e c = \gamma\beta$ is the normalized electron momentum, and $\gamma = (1+u^2)^{1/2} = (1-\beta^2)^{-1/2}$ is the relativistic factor. Here only the transverse focusing force of the plasma is considered. Near the axis, $r^2 \ll r_0^2$, the space charge potential is assumed to have the form

$$\hat{\Phi} = \hat{\Phi}_0(1 - r^2/r_0^2), \tag{4}$$

such that the normalized radial electric field is $\hat{E}_r = -\partial\hat{\Phi}/\partial r = 2\hat{\Phi}_0 r/r_0^2$, where $\hat{\Phi}_0$ and r_0 are constants. The electrostatic potential is related to the electron plasma density by

$\nabla^2\hat{\Phi} = k_p^2(n_e/n_0 - 1)$, where a uniform background of plasma ions of density n_0 is assumed. The maximum focusing field occurs when the plasma electrons are completely expelled (blown out) from the channel, $n_e = 0$. Notice that in the blowout regime, $\hat{E}_r = k_p^2 r/2$, hence, $\hat{\Phi}_0/r_0^2 \leq k_p^2/4$.

Equation (4) implies the existence of two constants of the motion, $du_z/dt = 0$ and $d(\gamma - \hat{\Phi})/dt = 0$. Inside the focusing channel, the electron orbits are given by

$$u_z = u_{z0}, \tag{5}$$

$$\gamma = \gamma_{z0} + \Delta\hat{\Phi}, \tag{6}$$

$$u_\perp^2 = 2\gamma_{z0}\Delta\hat{\Phi} + \Delta\hat{\Phi}^2, \tag{7}$$

where $\gamma_{z0} = (1 + u_{z0}^2)^{1/2}$, $\Delta\hat{\Phi} = \hat{\Phi}(r) - \hat{\Phi}(r_\beta)$, and r_β is the amplitude (assumed constant) of the betatron orbit. Note that at the maximum excursion of the betatron orbit, $u_\perp(r = r_\beta) = 0$. Assuming the electron orbit lies in the (x, z) plane, the orbit is given by

$$\tilde{\beta}_x \simeq k_\beta r_\beta \cos(k_\beta ct), \tag{8}$$

$$\tilde{x} \simeq r_\beta \sin(k_\beta ct), \tag{9}$$

$$\tilde{\beta}_z \simeq \beta_{z0}\left(1 - k_\beta^2 r_\beta^2/4\right) - \beta_{z0}(k_\beta^2 r_\beta^2/4)\cos(2k_\beta ct), \tag{10}$$

$$\tilde{z} \simeq z_0 + \beta_{z0}\left(1 - k_\beta^2 r_\beta^2/4\right)ct - \beta_{z0}(k_\beta^2 r_\beta^2/8)\sin(2k_\beta ct), \tag{11}$$

where

$$k_\beta = (2\hat{\Phi}_0/\gamma_{z0} r_0^2)^{1/2} \tag{12}$$

is the betatron wavenumber, $\beta_{z0} = u_{z0}/\gamma_{z0}$ and z_0 is a constant. Equations (8)-(11) are the leading order contributions to the orbits, assuming $k_\beta^2 r_\beta^2/2 \ll 1$. Notice that in the blowout regime $\hat{\Phi}_0 = k_p^2 r_0^2/4$, which gives $k_\beta = k_p/(2\gamma_{z0})^{1/2}$.

B. Electron Beam Envelope

For an ensemble of particles comprising an electron beam, the RMS beam radius r_b evolves via the envelope equation [33]

$$d^2 r_b/dct^2 = \epsilon_n^2 \gamma^{-2} r_b^{-3} - k_\beta^2 r_b, \tag{13}$$

where $\epsilon_n \simeq \gamma r_b \theta_b$ is the normalized beam emittance and θ_b is the RMS beam angle, where the effects of finite energy spread and space charge have been neglected. The solution to Eq. (13) for $r_b(ct)$ with $r_b = r_i$ (injected beam radius) and $dr_b/dct = 0$ at $ct = 0$ is given by

$$2\frac{r_b^2}{r_i^2} = \left(1 + \frac{\epsilon_n^2}{\gamma^2 k_\beta^2 r_i^4}\right) + \left(1 - \frac{\epsilon_n^2}{\gamma^2 k_\beta^2 r_i^4}\right) \cos(2k_\beta ct). \tag{14}$$

The matched beam radius $r_b = r_i = r_{bm}$ for which $d^2 r_b/dct^2 = 0$ is $r_{bm} = (\epsilon_n/\gamma k_\beta)^{1/2}$, at which point the expansion of the beam due to finite emittance is balanced by the focusing forces of the plasma channel. For parameters typical of the E-157 experiment ($\epsilon_n = 10$ mm-mrad, $\gamma = 6 \times 10^4$, and $\lambda_\beta = 0.82$ m), $r_{bm} = 4.7$ μm. If the beam is not matched within the channel, the beam radius oscillates between $r_b^2 = r_i^2$ and $r_b^2 = \epsilon_n^2/(\gamma^2 k_\beta^2 r_i^2) = r_{bm}^4/r_i^2$ with period $\lambda_{osc} = \pi/k_\beta = \lambda_\beta/2$ and having an average value $\langle r_b^2 \rangle = (r_i^2/2)(1 + r_{bm}^4/r_i^4)$.

III. SYNCHROTRON RADIATION

The energy spectrum of the radiation emitted by a single electron on an arbitrary orbit $\tilde{\mathbf{r}}(t)$ and $\tilde{\beta}(t)$ can be calculated from the Lienard-Wiechert potentials [34],

$$\frac{d^2 I}{d\omega d\Omega} = \frac{e^2\omega^2}{4\pi^2 c}\left| \int_{-T/2}^{T/2} dt \left[\mathbf{n} \times (\mathbf{n} \times \tilde{\beta})\right] \exp\left[i\omega(t - \mathbf{n}\cdot\tilde{\mathbf{r}}/c)\right] \right|^2, \tag{15}$$

where $d^2 I/d\omega d\Omega$ is the energy radiated per frequency, ω, per solid angle, Ω, during the interaction time, T, and $\mathbf{n}$ is a unit vector pointing in the direction of observation. Using the betatron orbits given above, the radiation spectrum can be calculated with conventional techniques [36] - [38]. It is convenient to introduce spherical coordinates (r, θ, ϕ) and unit vectors $(\mathbf{e}_r, \mathbf{e}_\theta, \mathbf{e}_\phi)$, where $x = r\sin\theta\cos\phi$, $y = r\sin\theta\sin\phi$, $z = r\cos\theta$, and

$$\mathbf{e}_r = \sin\theta\cos\phi\ \mathbf{e}_x + \sin\theta\sin\phi\ \mathbf{e}_y + \cos\theta\ \mathbf{e}_z, \tag{16}$$

$$\mathbf{e}_\theta = \cos\theta\cos\phi\ \mathbf{e}_x + \cos\theta\sin\phi\ \mathbf{e}_y - \sin\theta\ \mathbf{e}_z, \tag{17}$$

$$\mathbf{e}_\phi = -\sin\phi\ \mathbf{e}_x + \cos\phi\ \mathbf{e}_y. \tag{18}$$

Identifying $\mathbf{e}_r = \mathbf{n}$, gives

$$\mathbf{n}\times(\mathbf{n}\times\tilde{\beta}) = -(\tilde{\beta}_x\cos\theta\cos\phi + \tilde{\beta}_y\cos\theta\sin\phi - \tilde{\beta}_z\sin\theta)\ \mathbf{e}_\theta$$

$$+(\tilde{\beta}_x\sin\phi - \tilde{\beta}_y\cos\phi)\ \mathbf{e}_\phi, \tag{19}$$

$$\mathbf{n}\cdot\tilde{\mathbf{r}} = \tilde{x}\sin\theta\cos\phi + \tilde{y}\sin\theta\sin\phi + \tilde{z}\cos\theta. \tag{20}$$

The scattered radiation will be polarized in the direction of $\mathbf{n}\times(\mathbf{n}\times\tilde{\beta})$. Hence, $I = I_\theta + I_\phi$, where I_θ and I_ϕ are the energies radiated with polarizations in the $\mathbf{e}_\theta$ and $\mathbf{e}_\phi$ directions, respectively, i.e.,

$$\frac{d^2I_\theta}{d\omega d\Omega} = \frac{e^2\omega^2}{4\pi^2c^3}\left|\int_{-T/2}^{T/2} dt\left(\frac{d\tilde{x}}{dt}\cos\theta\cos\phi + \frac{d\tilde{y}}{dt}\cos\theta\sin\phi - \frac{d\tilde{z}}{dt}\sin\theta\right)\exp(i\psi)\right|^2, \tag{21}$$

$$\frac{d^2I_\phi}{d\omega d\Omega} = \frac{e^2\omega^2}{4\pi^2c^3}\left|\int_{-T/2}^{T/2} dt\left(\frac{d\tilde{x}}{dt}\sin\phi - \frac{d\tilde{y}}{dt}\cos\phi\right)\exp(i\psi)\right|^2, \tag{22}$$

where

$$\psi = (\omega/c)\left(ct - \tilde{z}\cos\theta - \tilde{x}\sin\theta\cos\phi - \tilde{y}\sin\theta\sin\phi\right). \tag{23}$$

In the following, the electron orbit is assumed to reside in the (x,z) plane, and is given by Eqs. (8)-(11). Hence,

$$\psi = \psi_0 + \alpha_0 kct - \alpha_x\sin k_\beta ct + \alpha_z\sin 2k_\beta ct, \tag{24}$$

$$\alpha_0 = 1 - \beta_{z0}(1 - k_\beta^2 r_\beta^2/4)\cos\theta, \tag{25}$$

$$\alpha_x = kr_\beta\sin\theta\cos\phi, \tag{26}$$

$$\alpha_z = \beta_{z0}(kk_\beta r_\beta^2/8)\cos\theta, \tag{27}$$

where $k = \omega/c$ and $\psi_0 = -kz_0\cos\theta$. Using the identity

$$\exp(ib\sin\sigma) = \sum_{n=-\infty}^{\infty} J_n(b)\exp(in\sigma), \tag{28}$$

where J_n are Bessel functions, allows the phase factor $\exp\left[i(\psi+\ell k_\beta ct)\right]$ to be written as

$$\exp\left[i(\psi+\ell k_\beta ct)\right]=\sum_{m,n=-\infty}^{\infty}J_m(\alpha_z)J_{n+2m+\ell}(\alpha_x)\exp\left[i(\psi_0+\bar{k}ct)\right], \tag{29}$$

where

$$\bar{k}=\alpha_0 k-nk_0. \tag{30}$$

In order to evaluate Eqs. (21) and (22), it is necessary to evaluate the integrals

$$\hat{I}_{(x,z)}=\int_{-T/2}^{T/2}dt\frac{d(\tilde{x},\tilde{z})}{dt}\exp(i\psi). \tag{31}$$

Using the orbits, Eqs. (8)-(11), along with the identities in Eqs. (28) and (29), gives

$$\hat{I}_x=k_\beta r_\beta e^{i\psi_0}\sum_{m,n=-\infty}^{\infty}\left(\frac{\sin\bar{k}L/2}{\bar{k}}\right)J_m(\alpha_z)\left[J_{n+2m-1}(\alpha_x)+J_{n+2m+1}(\alpha_x)\right], \tag{32}$$

$$\begin{aligned}\hat{I}_z=\beta_{z0}e^{i\psi_0}&\sum_{m,n=-\infty}^{\infty}\left(\frac{\sin\bar{k}L/2}{\bar{k}}\right)J_m(\alpha_z)\\&\times\left\{2\left(1-\frac{k_b^2r_b^2}{4}\right)J_{n+2m}(\alpha_z)-\frac{k_\beta^2r_\beta^2}{4}\left[J_{n+2m-2}(\alpha_x)+J_{n+2m+2}(\alpha_x)\right]\right\},\end{aligned} \tag{33}$$

where $L=cT$ and

$$\frac{d^2I_\theta}{d\omega d\Omega}=\frac{e^2\omega^2}{4\pi^2c^3}\left|\hat{I}_x\cos\theta\cos\phi-\hat{I}_z\sin\theta\right|^2, \tag{34}$$

$$\frac{d^2I_\phi}{d\omega d\Omega}=\frac{e^2\omega^2}{4\pi^2c^3}\left|\hat{I}_x\sin\phi\right|^2. \tag{35}$$

Assuming that the frequency spectra for two different harmonics, n and n', are sufficiently well separated, the summations in Eqs. (34) and (35) may be simplified to yield

$$\begin{aligned}\frac{d^2I}{d\omega d\Omega}=&\sum_{n=1}^{\infty}\frac{e^2k^2}{4\pi^2c}\left(\frac{\sin\bar{k}L/2}{\bar{k}}\right)^2\\&\times\left[C_x^2(1-\sin^2\theta\cos^2\phi)+C_z^2\sin^2\theta-C_xC_z\sin2\theta\cos\phi\right],\end{aligned} \tag{36}$$

where

$$C_x=k_\beta r_\beta\sum_{m=-\infty}^{\infty}J_m(\alpha_z)\left[J_{n+2m-1}(\alpha_x)+J_{n+2m+1}(\alpha_x)\right], \tag{37}$$

$$C_z=\beta_{z0}\sum_{m=-\infty}^{\infty}J_m(\alpha_z)\{2(1+k_\beta^2r_\beta^2/4)J_{n+2m}(\alpha_x)$$

$$- (k_\beta^2 r_\beta^2/4)\left[J_{n+2m-2}(\alpha_x) + J_{n+2m+2}(\alpha_x)\right]\}, \tag{38}$$

$$\alpha_z = \frac{n(k/k_n)(a_\beta^2/4)\cos\theta}{\left[(1+a_\beta^2/2)\cos\theta + 2\gamma_{z0}^2(1-\cos\theta)\right]}, \tag{39}$$

$$\alpha_x = \frac{n(k/k_n)2\gamma_{z0}a_\beta\sin\theta\cos\phi}{\left[(1+a_\beta^2/2)\cos\theta + 2\gamma_{z0}^2(1-\cos\theta)\right]}, \tag{40}$$

and

$$a_\beta = \gamma_{z0}k_\beta r_\beta \tag{41}$$

is the betatron strength parameter. Here, $L = cT$ is the interaction length, $k = \omega/c$ is the radiation wavenumber, n is the harmonic number, and J_m are Bessel functions. For parameters typical of the E-157 experiment ($\gamma = 6\times10^4$ and $\lambda_\beta = 0.82$ m), $a_\beta = 45$ for $r_\beta = r_b = 100$ μm (typical unmatched beam radius) and $a_\beta = 2.1$ for $r_\beta = r_{bm} = 4.7$ μm (typical matched beam radius).

In the limits $\gamma_{z0}^2 \gg 1$, $\theta^2 \ll 1$, and $a_\beta^2/\gamma_{z0}^2 \ll 1$, the radiation spectrum can be written as

$$\frac{d^2I}{d\hbar\omega d\Omega} = \sum_{n=1}^{\infty}\alpha_f\gamma_{z0}^2\hat{k}^2N_\beta^2R_n\left[\gamma_{z0}^2C_x^2 + C_z^2\hat{\theta}^2 - 2\gamma_{z0}C_xC_z\hat{\theta}\cos\phi\right], \tag{42}$$

where

$$\gamma_{z0}C_x = a_\beta\sum_{m=-\infty}^{\infty}J_m(\alpha_z)\left[J_{n+2m-1}(\alpha_x) + J_{n+2m+1}(\alpha_x)\right], \tag{43}$$

$$C_z = \sum_{m=-\infty}^{\infty}2J_m(\alpha_z)J_{n+2m}(\alpha_x), \tag{44}$$

$$\alpha_z = \frac{n(\hat{k}/\hat{k}_n)(a_\beta^2/4)}{(1+a_\beta^2/2+\hat{\theta}^2)}, \tag{45}$$

$$\alpha_x = \frac{n(\hat{k}/\hat{k}_n)(2a_\beta)\hat{\theta}\cos\phi}{(1+a_\beta^2/2+\hat{\theta}^2)}, \tag{46}$$

and

$$R_n = \frac{\sin^2\left[\pi nN_\beta(\hat{k}/\hat{k}_n - 1)\right]}{\left[\pi nN_\beta(\hat{k}/\hat{k}_n - 1)\right]^2} \tag{47}$$

is the resonance function, with $N_\beta = L/\lambda_\beta$ the number of betatron periods that the electron undergoes and $\alpha_f = e^2/\hbar c \simeq 1/137$ the fine structure constant. Here $\hat{\theta} = \gamma_{z0}\theta$ and the normalized frequencies are $\hat{k} = k/2\gamma_{z0}^2k_\beta$ and $\hat{k}_n = k_n/2\gamma_{z0}^2k_\beta = n/(1+a_\beta^2/2+\hat{\theta}^2)$.

Plots of the normalized intensity distributions $d^2I/d\hbar\omega d\Omega$ for the first four harmonics ($n = 1, 2, 3$ and 4) from a single electron is shown in Fig. 2 for $a_\beta = 2$ in the limit $N_\beta \gg 1$ such that $k = k_n$ in Eqs. (42)-(47). The intensity distribution is plotted in the transverse plane (x, y) of a detector located along the z-axis some large distance z ($x/z \sim y/z \sim 1/\gamma_{z0}$) from the interaction, where $\hat{x} = \gamma_{z0}x/z$, $\hat{y} = \gamma_{z0}y/z$, $\hat{\theta} = (\hat{x}^2 + \hat{y}^2)^{1/2}$, and $\cos\phi = \hat{x}/\hat{\theta}$. The color coding shows the resonant frequency of the scattered radiation $\hat{k}_n = n/(1 + a_\beta^2/2 + \hat{\theta}^2)$.

A. Resonance Function

Provided the number of betatron periods is large, $N_\beta \gg 1$, radiation is emitted in a series of harmonics and is confined in a narrow bandwidth about the resonant frequency of each harmonic. The frequency width of the radiation spectrum for a given harmonic is determined by the resonance function $R_n(k)$, where

$$R_n(k) = \left(\frac{\sin \bar{k}L/2}{\bar{k}L/2}\right)^2. \tag{48}$$

This function is sharply peaked about the resonant frequency, $\omega_n = ck_n$, given by $\bar{k} = 0$,

$$k_n = \frac{nk_\beta}{\alpha_0} \simeq \frac{2\gamma_{z0}^2 nk_\beta}{\left[(1 + a_\beta^2/2)\cos\theta + 2\gamma_{z0}^2(1 - \cos\theta)\right]}, \tag{49}$$

where $\gamma_{z0}^2 \gg 1$ was assumed. Typically, for frequencies of interest, the synchrotron radiation is confined to a cone angle $\theta^2 \ll 1$ and the resonant frequency can be approximated by

$$\omega_n \simeq nM_0 ck_\beta/(1 + M_0\theta^2/2), \tag{50}$$

where $M_0 = 2\gamma_{z0}^2/(1+a_\beta^2/2)$ is the relativistic Doppler upshift factor. The intrinsic frequency width $\Delta\omega_n$ of the spectrum R_n about ω_n is given by $\Delta\omega_n/\omega_n = 1/nN_\beta$. Furthermore, $R_n(k) \to \Delta\omega_n\delta(\omega - \omega_n)$ as $N_\beta \to \infty$. For a single harmonic n, the angular width $\Delta\theta_I$ about the axis of a cone containing radiation with frequencies in a small bandwidth $\Delta\omega$ about ω_n is given by

$$\Delta\theta_I^2 \simeq \left(\frac{2}{M_0}\right) \times \begin{cases} \Delta\omega_n/\omega_n & \text{for } \Delta\omega \le \Delta\omega_n, \\ \Delta\omega/\omega_n & \text{for } \Delta\omega \ge \Delta\omega_n. \end{cases} \tag{51}$$

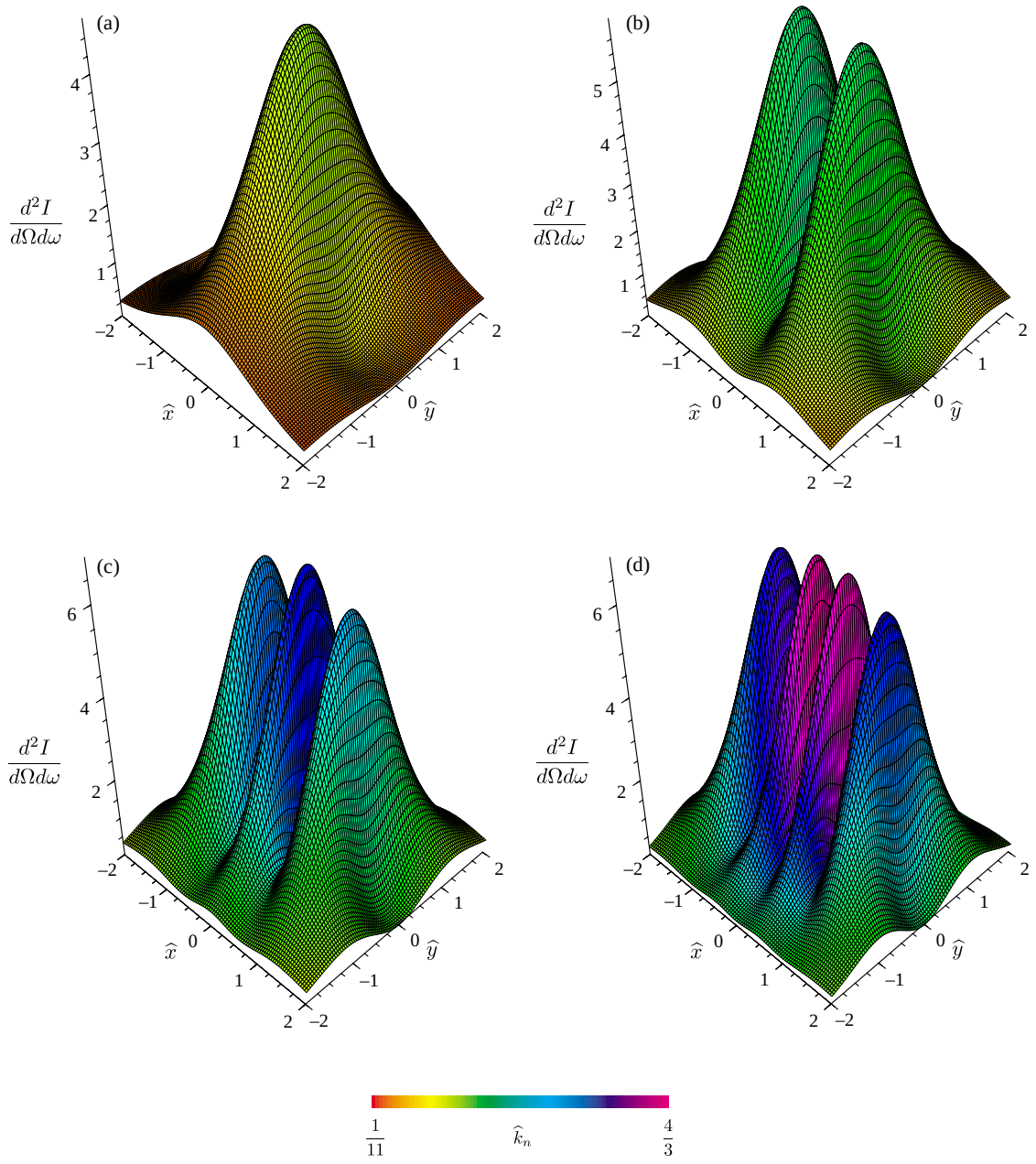

FIG. 2. Intensity distributions (arbitrary units) in the $\hat{x} = \gamma_{z0}x/z$ and $\hat{y} = \gamma_{z0}y/z$ plane for the first four harmonics $n = 1$ (upper left), 2, 3, and 4 (lower right) for $a_\beta = 2$. The distributions are evaluated at the normalized resonant frequency $\hat{k} = \hat{k}_n = n/(1 + a_\beta^2/2 + \hat{\theta}^2)$, the value of which is indicated by the color scale.

B. On-Axis Radiation

Of particular interest is the radiation emitted along the axis, $\theta = 0$, where only the odd harmonics are finite, i.e., the even harmonics vanish. Setting $\theta = 0$ in the above expressions gives, for the n^{th} odd harmonic, $\alpha_x = 0$, $\alpha_z = \alpha_n$, and

$$\frac{d^2 I_n(0)}{d\omega d\Omega} = 2e^2 \frac{\omega}{\omega_n} k_\beta N_\beta M_0^2 G_n F_n = \frac{4e^2}{c} \frac{\omega}{\omega_n} \frac{\gamma_{z0}^2 N_\beta^2 R_n F_n}{(1 + a_\beta^2/2)}, \tag{52}$$

where

$$F_n(a_\beta) = n\alpha_n \left[J_{(n-1)/2}(\alpha_n) - J_{(n+1)/2}(\alpha_n) \right]^2 \tag{53}$$

is the harmonic amplitude function,

$$\alpha_n = \frac{n(\omega/\omega_n) a_\beta^2/4}{(1 + a_\beta^2/2)}, \tag{54}$$

and

$$G_n(\omega) = \frac{R_n(k)}{\Delta\omega_n} = \frac{1}{\Delta\omega_n} \frac{\sin^2[\pi n N_\beta(\omega/\omega_n - 1)]}{[\pi n N_\beta(\omega/\omega_n - 1)]^2} \tag{55}$$

is the frequency spectrum function with the resonant frequency $\omega_n = nM_0 c k_\beta$.

An expression for the number of photons (N_n) radiated along the axis per solid angle, $dN_n/d\Omega$, per electron for photons in a narrow bandwidth $\Delta\omega$ about the resonant frequency ω_n is obtained by integrating Eq. (52) over $\Delta\omega$ and by dividing for the energy per photon ($\hbar\omega_n$),

$$\frac{dN_n}{d\Omega} \simeq 4\alpha_f \frac{\Delta\omega_I}{\omega_n} \frac{\gamma_{z0}^2 N_\beta^2 F_n}{(1 + a_\beta^2/2)}, \tag{56}$$

where $\Delta\omega_I = \Delta\omega$ for $\Delta\omega \leq \Delta\omega_n$ and $\Delta\omega_I = \Delta\omega_n$ for $\Delta\omega \geq \Delta\omega_n$, with $\Delta\omega_n = \omega_n/nN_\beta$ the intrinsic bandwidth and α_f the fine structure constant. The total number of photons radiated per electron in the bandwidth $\Delta\omega$ about ω_n is given by multiplying $dN_n/\Delta\Omega$ by the solid angle $2\pi(\Delta\theta_I^2/2)^{1/2}$, where $\Delta\theta_I$ is given by Eq. (51). This yields

$$N_n \simeq 4\pi\alpha_f (\Delta\omega/\omega_n)(N_\beta/n) F_n(a_\beta), \tag{57}$$

for all values of $\Delta\omega^2 \ll \omega_n^2$.

The photon angular density $dN_n/d\Omega$ and the spectral energy density $d^2I(0)/d\omega d\Omega$ of the n^{th} harmonic emitted along the axis are both proportional to the function $F_n/(1+a_\beta^2/2)^{1/2}$. The number of photons radiated in the n^{th} harmonic along the axis depends on the function F_n/n. For high harmonics, $n \gg 1$, F_n becomes significant when $a_\beta^2 \gg 1$. For $a_\beta^2 \ll 1$, only the fundamental, $n = 1$, is significant. A plot of $F_n/(1 + a_\beta^2/2)$ (top) and F_n/n (bottom) versus $\alpha_n/n = (a_\beta^2/4)/(1 + a_\beta^2/2)$ is shown in Fig. 3 for the first eight odd harmonics, where $n = 1$ is the uppermost curve and $n = 15$ is the lowermost curve.

C. Ultra-Intense Behavior

For values of $a_\beta^2 \ll 1$, the scattered radiation will be narrowly peaked about the fundamental resonant frequency, ω_1, given by Eq. (50) with $n = 1$. As a_β approaches unity, scattered radiation will appear at harmonics of the resonant frequency as well, $\omega_n = n\omega_1$. When $a_\beta \gg 1$, high harmonic ($n \gg 1$) radiation is generated and the resulting synchrotron radiation spectrum consists of many closely spaced harmonics. Finite variations in the parameter $a_\beta = \gamma_{z0} k_\beta r_\beta$ within an electron beam can broaden the linewidth and cause the spectrum to overlap. Hence, in the ultra-intense limit, i.e., $a_\beta \gg 1$, the gross spectrum appears broadband, and a continuum of radiation is generated which extends out to a critical frequency, ω_c, beyond which the radiation intensity diminishes. The critical frequency can be written as $\omega_c = n_c M_0 \omega_\beta$, where n_c is the critical harmonic number. It is possible to calculate n_c by examining the radiation spectrum, Eq. (36), in the ultra-intense limit, $a_\beta \gg 1$.

Furthermore, when $a_\beta \ll 1$, radiation is generated in a narrow cone about the backscatter direction, $\Omega \simeq 2\pi\theta_c^2$, where $\theta_c \sim 1/\gamma_{z0}$. However, when $a_\beta \gg 1$, the emission cone about backscatter direction widens. In particular, in the vertical direction, $\phi = \pi/2$ (the direction normal to the x-z plane which contains the electron orbit), emission is confined to the vertical angle $\theta_v \sim 1/\gamma_{z0}$. In the horizontal direction, $\phi = 0$ (in the plane of the electron orbit), the emission angle widens and is confined the horizontal angle $\theta_h \sim a_0/\gamma_{z0}$, which is determined

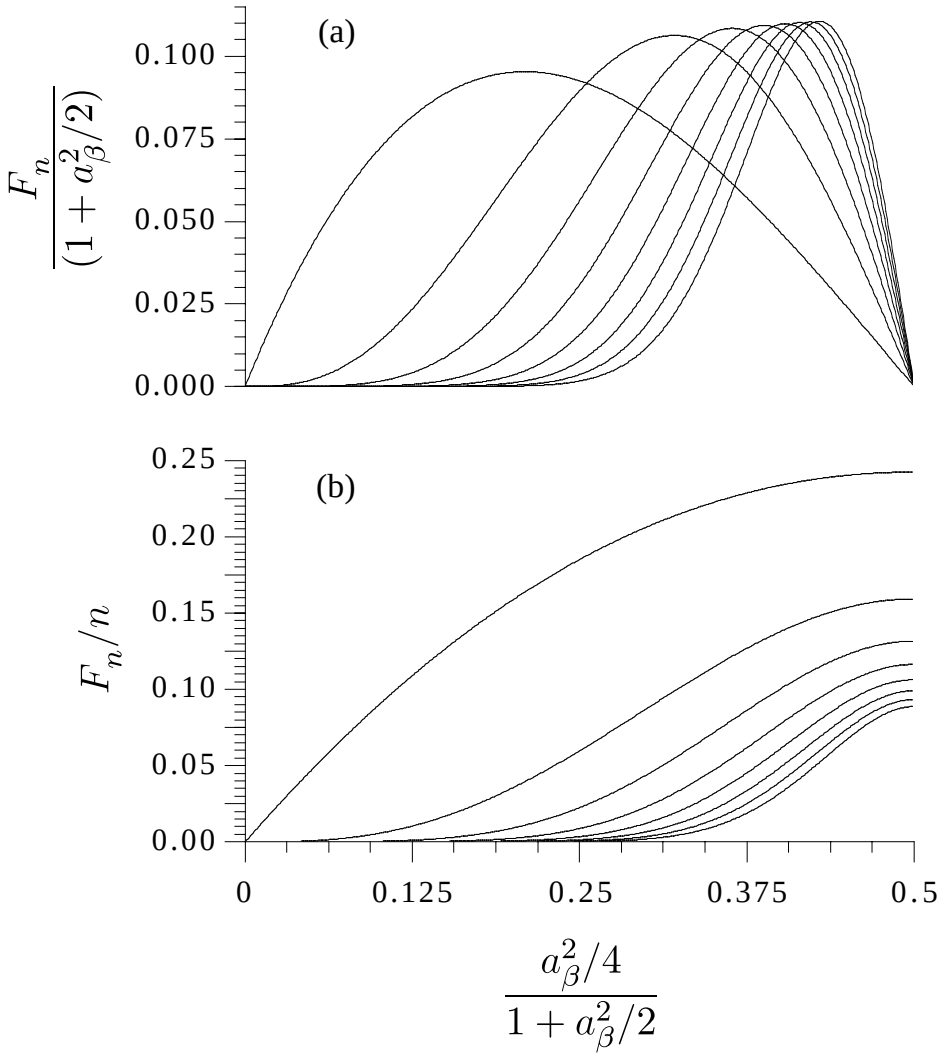

FIG. 3. The functions $F_n/(1+a_\beta^2/2)$ (top) and F_n/n (bottom) versus $\alpha_n/n = (a_\beta^2/4)/(1+a_\beta^2/2)$ for the first eight odd harmonics, where $n = 1$ is the leftmost curve and $n = 15$ is the rightmost curve.

by the deflection angle of the electron in the x-z plane.

Asymptotic properties of the radiation spectrum for large harmonic numbers, $n \gg 1$, can be analyzed using the relationships [39]

$$J_n(n\hat{z}) \simeq \frac{\hat{x}^{1/2}}{\pi}(1-\hat{z}^2)^{-1/4}K_{1/3}(n\hat{x}), \tag{58}$$

$$J_n'(n\hat{z}) \simeq -\frac{\hat{x}^{1/2}}{\pi\hat{z}}(1-\hat{z}^2)^{1/4}K_{2/3}(n\hat{x}), \tag{59}$$

where $|\hat{z}| < 1$ and is a function of a_β and θ,

$$\hat{x} = \ln\left[1+(1-\hat{z}^2)^{1/2}\right] - \ln\hat{z} - (1-\hat{z}^2)^{1/2}, \tag{60}$$

and $K_{1/3}$, $K_{2/3}$ are modified Bessel functions. In particular, for $n\hat{x} \gg 1$,

$$K_{1/3} \simeq K_{2/3} \simeq (\pi/2n\hat{x})\exp(-n\hat{x}), \tag{61}$$

and, hence, only harmonic radiation with $n\hat{x} \lesssim 1$ will contribute significantly to the spectrum. The critical harmonic number is defined as $n_c\hat{x}_{min} = 1$, i.e., $n_c = 1/\hat{x}_{min}$, where $\hat{x}_{min}$ is the minimum value of Eq. (60). Furthermore, $d\hat{x}/d\hat{z} < 0$ and the minimum of $\hat{x}$ occurs at $\hat{z}_{max}$. Typically, for $a_\beta^2 \gg 1$, $1-\hat{z}_{max}^2 \ll 1$ and Eq. (60) can be expanded to yield, to leading order, $\hat{x}_{min} \simeq (1/3)\,(1-\hat{z}_{max}^2)^{3/2}$. The critical harmonic number is given by the inverse of this expression.

Letting θ represent the observation angle in the vertical direction (i.e., $\phi = \pi/2$), then in the limits $a_\beta \gg 1$, $n \gg 1$, and $\theta^2 \ll 1$, the coefficients C_x and C_z occurring in Eq. (36) are given by $C_z^2 \simeq 4J_\ell^2(\ell\hat{z})$ and $C_x^2 \simeq k_\beta^2 r_\beta^2 J_\ell'^2(\ell\hat{z})$, where additional terms of order $1/a_\beta$ have been neglected and $n = 2\ell+1 \gg 1$. Here,

$$\hat{z} = \frac{\alpha_z}{\ell} \simeq \frac{a_\beta^2/2}{1+a_\beta^2/2+\gamma_{z0}^2\theta^2}. \tag{62}$$

Note that $1-\hat{z}^2 \simeq (4/a_\beta^2)(1+\gamma_{z0}^2\theta^2)$, assuming $a_\beta^2 \gg 1+\gamma_{z0}^2\theta^2$. Hence, for $\theta = 0$, $\hat{x}_{max} = 1/\ell_c \simeq 8/3a_\beta^3$, and the critical harmonic number, $n_c \simeq 2\ell_c$ is

$$n_c \simeq 3a_\beta^3/4. \tag{63}$$

Using Eqs. (36), (58) and (59), the asymptotic spectrum in the vertical direction is

$$\frac{d^2I}{d\omega d\Omega} \simeq N_\beta \frac{6e^2}{\pi^2 c} \frac{\gamma_{z0}^2 \zeta^2}{(1+\gamma_{z0}^2\theta^2)} \left[\frac{\gamma_{z0}^2\theta^2}{(1+\gamma_{z0}^2\theta^2)} K_{1/3}^2(\zeta) + K_{2/3}^2(\zeta) \right], \tag{64}$$

where

$$\zeta = \frac{\omega}{\omega_c}(1+\gamma_{z0}^2\theta^2)^{3/2}, \tag{65}$$

$$\omega_c = n_c M_0 \omega_\beta \simeq 3 a_\beta \gamma_{z0}^2 \omega_\beta, \tag{66}$$

is the critical frequency, and $M_0 \simeq 4\gamma_{z0}^2/a_\beta^2$. In deriving Eq. (64), $\ell\hat{x} \rightarrow \zeta$ and $\sum_n R(k, nk_0) \rightarrow 1/2N_\beta$, where the factor of 1/2 is due to the fact that in the asymptotic limit, $n \simeq 2\ell$. For E-157-like parameters ($\gamma = 6 \times 10^4$, $\lambda_\beta = 0.82$ m, and $a_\beta = 45$), $n_c \simeq 6.8 \times 10^4$ and $\lambda_c = 2\pi c/\omega_c \simeq 1.7 \times 10^{-12}$ m. Hence, for these parameters, the radiation spectrum can be accurately described by the asymptotic expressions, Eqs. (64)-(66).

Along the axis $\theta = 0$, $d^2I(0)/d\omega d\Omega \sim \xi^2 K_{2/3}^2(\xi)$, where $\xi = \omega/\omega_c$. The function $Y(\xi) = \xi^2 K_{2/3}^2(\xi)$ is maximum at $\xi = 1/2$ and decreases rapidly for $\xi > 1$. A plot of the function $Y(\xi)$ versus $\omega/2\gamma_{z0}^2\omega_\beta$ is shown in Fig. 4 (top plot - linear scale; bottom plot - log scale). The solid curve shows the radiation from a single electron with $a_\beta = \gamma_{z0} k_\beta r_\beta = 10$. The dashed curve shows the $Y(\xi)$ spectrum integrated over a Gaussian distribution of betatron amplitudes r_β (i.e., an electron beam with a Gaussian radial profile, as is discussed in the following section) with a rms value satisfying $a_{\beta,rms} = \gamma_{z0} k_\beta r_{\beta,rms} = 10$. To calculate these averages, the quantity $\xi = \omega/\omega_c$ has been approximated by $\xi \simeq (\omega/2\gamma_{z0}^2\omega_\beta)(1+3a_\beta/2)^{-1}$, since the asymptotic form for the spectrum is not accurate when $a_\beta < 1$, i.e., the dashed curve in Fig. 4 is inaccurate in the region $\omega/2\gamma_{z0}^2\omega_\beta \lesssim 1$.

Equation (64) is analogous with $2N_\beta$ [34] for the synchrotron radiation spectrum emitted from an electron moving in an instantaneously circular orbit in the ultra-relativistic limit with a radius of curvature $\rho = 3\gamma_{z0}^3 c/\omega_c$. Several well-known properties [34] follow from Eq. (64), for example

$$\frac{dI}{d\Omega} \simeq \frac{7e^2}{24c} \frac{N_\beta \omega_c \gamma_{z0}^2}{(1+\gamma_{z0}^2\theta^2)^{5/2}} \left[1 + \frac{5}{7} \frac{\gamma_{z0}^2\theta^2}{(1+\gamma_{z0}^2\theta^2)} \right], \tag{67}$$

$$\frac{dI}{d\omega} \simeq 4\sqrt{3} \frac{e^2}{c} N_\beta \gamma_{z0} \frac{\omega}{\omega_c} \int_{2\omega/\omega_c}^{\infty} d\xi K_{5/3}(\xi). \tag{68}$$

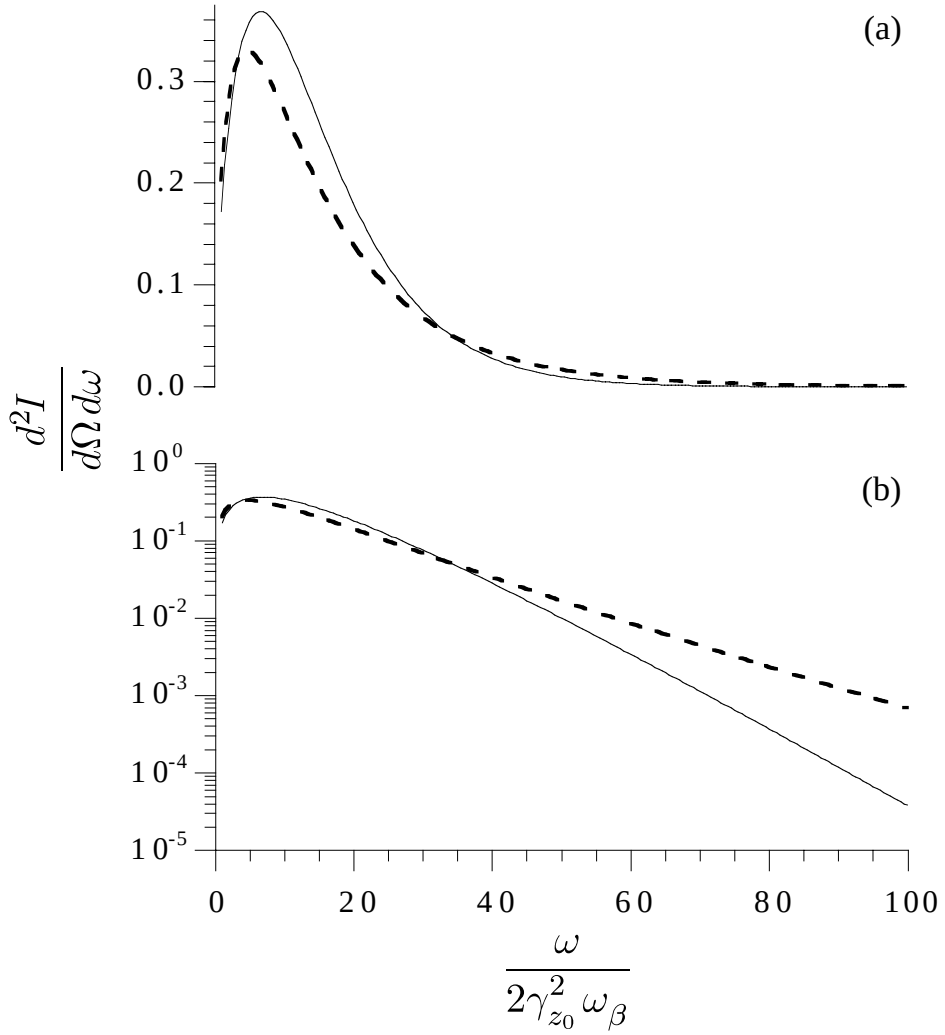

FIG. 4. The function $Y(\xi) = \xi^2 K_{2/3}^2(\xi)$ versus $\omega/2\gamma_{z0}^2\omega_\beta$ plotted on a linear (top) and log (bottom) scale. The solid curve shows the radiation from a single electron with $a_\beta = \gamma_{z0} k_\beta r_\beta = 10$. The dashed curve shows the spectrum integrated over a Gaussian distribution of betatron amplitudes r_β with $a_{\beta,rms} = \gamma_{z0} k_\beta r_{\beta,rms} = 10$.

The peak intensity is of the order $2N_\beta e^2\gamma_{z0}/c$ and the total radiated energy is of the order $2N_\beta e^2\gamma_{z0}\omega_c/c$. The peak intensity occurs at along the axis $\theta = 0$, at approximately the critical frequency, $\omega \simeq \omega_c$, i.e., $n \simeq n_c = 3a_\beta^3/4$. Half the total power is radiated at frequencies $\omega < \omega_c/2$ and half at $\omega > \omega_c/2$. For harmonics below n_c ($\omega \ll \omega_c$), the radiation intensity increases as $(\omega/\omega_0)^{2/3}$, and above n_c ($\omega \gg \omega_c$), the radiation intensity decreases exponentially as $\exp(-2\omega/\omega_c)$, i.e.,

$$\left.\frac{d^2I}{d\omega\delta\Omega}\right|_{\theta=0} \simeq N_\beta \frac{6e^2}{\pi^2 c}\left[\Gamma(2/3)\right]^2 \gamma_{z0}^2 \left(\frac{\omega}{2\omega_c}\right)^{2/3}, \quad \omega \ll \omega_c, \tag{69}$$

$$\left.\frac{d^2I}{d\omega\delta\Omega}\right|_{\theta=0} \simeq N_\beta \frac{3e^2}{\pi c}\gamma_{z0}^2 \left(\frac{\omega}{\omega_c}\right) \exp\left(-\frac{2\omega}{\omega_c}\right), \quad \omega \gg \omega_c. \tag{70}$$

Furthermore, for $\omega \ll \omega_c$, the scattered radiation at a fixed frequency is confined to an angular spread $\Delta\theta = (\omega_c/\omega)^{1/3}/\gamma_{z0}$ about $\theta = 0$, whereas for $\omega > \omega_c$, $\Delta\theta = (\omega_c/3\omega)^{1/2}/\gamma_{z0}$. The average angular spread for the frequency integrated spectrum in the vertical direction ($\phi = \pi/2$) is $\theta_v = \langle\theta^2\rangle^{1/2} \sim 1/\gamma_{z0}$. In the horizontal direction ($\phi = 0$), emission is confined to the angle $\theta_h \sim a_\beta/\gamma_{z0}$

IV. RADIATED POWER AND ELECTRON ENERGY LOSS

The power radiated by a single electron, P_s, undergoing relativistic motion in an arbitrary orbit can be calculated from the relativistic Larmor formula [34]

$$P_s = (2e^2/3c)\gamma^2\left[(d\mathbf{u}/dt)^2 - (d\gamma/dt)^2\right]. \tag{71}$$

Using the orbits described in Sec. II, the power radiated by a single electron undergoing betatron motion in a plasma focusing channel is

$$P_s \simeq (2/3) r_e m_e c^3 (1 + u_{z0}^2)\gamma_{z0}^2 k_\beta^4 \tilde{x}^2, \tag{72}$$

where $\tilde{x}$ is given by Eq. (9) and $r_e = e^2/m_e c^2$ is the classical electron radius. Averaging the above expression over a betatron period gives

$$\bar{P}_s \simeq r_e m_e c^3 \gamma_{z0}^2 k_\beta^2 a_\beta^2/3, \tag{73}$$

where $\gamma_{z0}^2 \gg 1$ was assumed.

The total energy radiated by a single electron W_s is given by the product of $\bar{P}_s$ with the interaction time $N_\beta \lambda_\beta / c$, i.e.,

$$W_s = (2\pi/3) r_e m_e c^2 \gamma_{z0}^2 k_\beta a_\beta^2 N_\beta. \tag{74}$$

The average number of photons radiated by a single electron $\langle N_s \rangle$ is given by dividing W_s by the average photon energy, $\hbar\langle\omega\rangle = 2\gamma_{z0}^2 \hbar\omega_\beta \langle n \rangle / (1 + a_\beta^2/2)$, i.e.,

$$\langle N_s \rangle = (\pi/3) \alpha_f (1 + a_\beta^2/2) a_\beta^2 N_\beta / \langle n \rangle, \tag{75}$$

where $\langle n \rangle$ is the average harmonic number and $\alpha_f = e^2/c\hbar$. In the limit $a_\beta^2 \ll 1$, $N_s \simeq \alpha_f N_\beta a_\beta^2$.

The rate at which a single electron loses energy due to radiating is $W'_{loss} = \bar{P}_s / c$, i.e.,

$$W'_{loss} \simeq r_e m_e c^2 \gamma_{z0}^2 k_\beta^2 a_\beta^2 / 3. \tag{76}$$

In the blowout regime, $k_\beta \sim n_0^{1/2} \gamma_{0z}^{-1/2}$, and the rate of energy loss scales as $W'_{loss} \sim n_0^2 \gamma_{z0}^2 r_\beta^2$. In addition, if the betatron amplitude is equal to the matched beam radius $r_b = (\epsilon_n / \gamma_{z0} k_\beta)^{1/2}$, the energy loss scales as $W'_{loss} \sim \epsilon_n \gamma_{z0}^3 k_\beta^3 \sim \epsilon_n n_0^{3/2} \gamma_{z0}^{3/2}$. For the parameters of the E-157 experiment in the blowout regime, i.e., a density $n_0 = 2 \times 10^{14}$ cm^{-3} ($\lambda_p = 0.24$ cm) and a beam energy of $\gamma_{z0} = 6 \times 10^4$, an electron with a betatron amplitude of $r_\beta = 100$ μm ($a_\beta = 45$) would lose energy at a rate of $W'_{loss} = 0.2$ MeV/m. This is small compared to the accelerating gradient in the E-157 experiment, which is several 100 MeV/m. This is a source of energy spread for the accelerated electrons, however, since an electron along the axis with $r_\beta = a_\beta = 0$ would not lose energy by this mechanism, i.e, the effective energy spread increases at a rate on the order of $\Delta W' \sim W'_{loss}$.

This radiative energy loss and the associated effective energy spread becomes more pronounced at higher density and energy, since $W'_{loss} \sim n_0^2 \gamma_{z0}^2 r_\beta^2$, whereas the accelerating field of the wake typically scales as $W'_{acc} \sim n_0^{1/2}$. For example, consider parameters relevant to experiments being planned at SLAC on the so-called "plasma afterburner" concept [35]. In

the plasma afterburner experiments, the energy of an initially 50 GeV electron bunch is increased by 56 GeV by passing the 63 μm long bunch through a 7 m long plasma of density 2×10^{16} cm^{-3} (100 times high density than the E-157 experiments). An electron of energy 100 GeV at the beam radius of $r_\beta = 25$ μm would have a betatron wavelength $\lambda_\beta \simeq 15$ m and a strength parameter of $a_\beta \simeq 210$. This gives an energy loss rate of $W'_{loss} \simeq 1.5$ GeV/m, which is a significant fraction ($\simeq 18\%$) of the predicted wakefield acceleration rate of 8 GeV/m.

V. RADIATION FROM A BEAM

For a single electron undergoing betatron motion in a plasma focusing channel, the resonant frequency of the radiation emitted along the axis is $\omega = 2\gamma_{z0}^2 n\omega_\beta/(1 + a_\beta^2/2)$, as indicated by Eq. (50). Here, $a_\beta = \gamma_{z0} k_\beta r_\beta$ is a function of both the electron energy γ_{z0} and the radial position of the electrons via the betatron amplitude r_β. If a monoenergetic beam of finite radius is injected into a focusing channel (without any special tapering), electrons at different radii will have different betatron amplitudes r_β, different values of a_β, and hence different resonant frequencies. In general, the spectral energy density of the radiation emitted by a finite radius beam will be significantly different from that of a single electron, especially in the limit $a_\beta \gtrsim 1$.

Consider the case of a monoenergetic, axisymmetric (round) beam in cylindrical geometry in the limit of zero emittance. In this case, $a_\beta = \gamma_{z0} k_\beta r_\beta$ represents the normalized radial position of the electron, since the initial radial position of the electron at the channel entrance is assumed to be equal to r_β. Let $d^2I/d\omega d\Omega = S_S(k, a_\beta, \theta, \phi)$ be the single-electron spectrum, as given by Eq. (42). The radiation spectrum from a beam, $S_B(k, \theta)$, can be approximately calculated from S_S by multiplying by the electron distribution function, f_e, and integrating over both radius (a_β) and over ϕ (from 0 to 2π for an axisymmetric beam). For an axisymmetric beam,

$$S_B(k, \theta) = \int_0^{2\pi} \frac{d\phi}{2\pi} \int_0^\infty da_\beta a_\beta f_e(a_\beta) S_S(k, a_\beta, \theta, \phi). \tag{77}$$

For simplicity, a Gaussian radial beam distribution $f_e(a_\beta)$ is assumed

$$f_e(r_\beta) = f_e(a_\beta) = (2/a_{rms}^2)\exp(-a_\beta^2/a_{rms}^2), \tag{78}$$

such that $\int_0^\infty da_\beta a_\beta f_e = 1$ and $\int_0^\infty da_\beta a_\beta^3 f_e = a_{rms}^2$, where a_{rms} is the normalized RMS beam radius, $a_{rms} = \gamma_{z0} k_\beta r_b$.

For a large number of betatron periods, the radial integration can be approximated analytically. Let

$$S_R = \int_0^\infty da_\beta a_\beta f_e S_S = \int_0^\infty da_\beta a_\beta f_e \hat{S}_S R_n(k, a_\beta, \theta), \tag{79}$$

where R_n is the resonance function given by Eq. (48). At resonance $k = k_n(a_\beta)$ or, alternatively, $a_\beta = a_r(k)$, where

$$a_r^2 = 2\left[n2\gamma_{z0}^2 k_\beta/k - (1+\gamma_{z0}^2\theta^2)\right]. \tag{80}$$

Furthermore, in the limit $N_\beta \to \infty$, $R_n \to \Delta a_\beta \delta(a_\beta - a_r)$, where $\Delta a_\beta = 2\gamma_{z0}^2 k_\beta / N_\beta a_\beta k_\beta$. Hence, for $N_\beta \to \infty$, $S_S \simeq \hat{S}_S \Delta a_\beta \delta(a_\beta - a_r)$ and

$$S_R \simeq \frac{2\gamma_{z0}^2 k_\beta}{N_\beta k} f_e(a_\beta = a_r)\hat{S}_S(a_\beta = a_r). \tag{81}$$

In this limit, the spectrum of the radiation emitted along the axis ($\theta = 0$) from a Gaussian beam profile is

$$S_B(\theta = 0) = \sum_n (4e^2/c)\gamma_{z0}^2 N_\beta f_e(a_r) F_n(a_r)/n, \tag{82}$$

where sum is over odd harmonics n and $F_n(a_r)$ is given by Eq. (53) evaluated at $a_\beta^2 = a_r^2 = 2(n/\hat{k} - 1)$, i.e., the argument of the Bessel functions is $\alpha_n = (n - \hat{k})/2$, where $\hat{k} = k/2\gamma_{z0}^2 k_\beta$. This is to be compared with Eq. (52), which gives the on-axis spectrum for a single electron.

Figure 5 shows a plot of $d^2I(0)/d\omega\delta\Omega$ versus $\omega/2\gamma_{z0}^2\omega_\beta$ for the first several odd harmonics with $N_\beta = 4$. The solid curve shows the radiation from a single electron with $a_\beta = 2$, as obtained from Eq. (52), indicating that radiation is emitted in well-defined harmonics. The dashed curve shows the spectrum for a beam with a Gaussian radial distribution with $a_{rms} = 2$, as obtained from Eq. (82). The effect of averaging over a distribution of electron

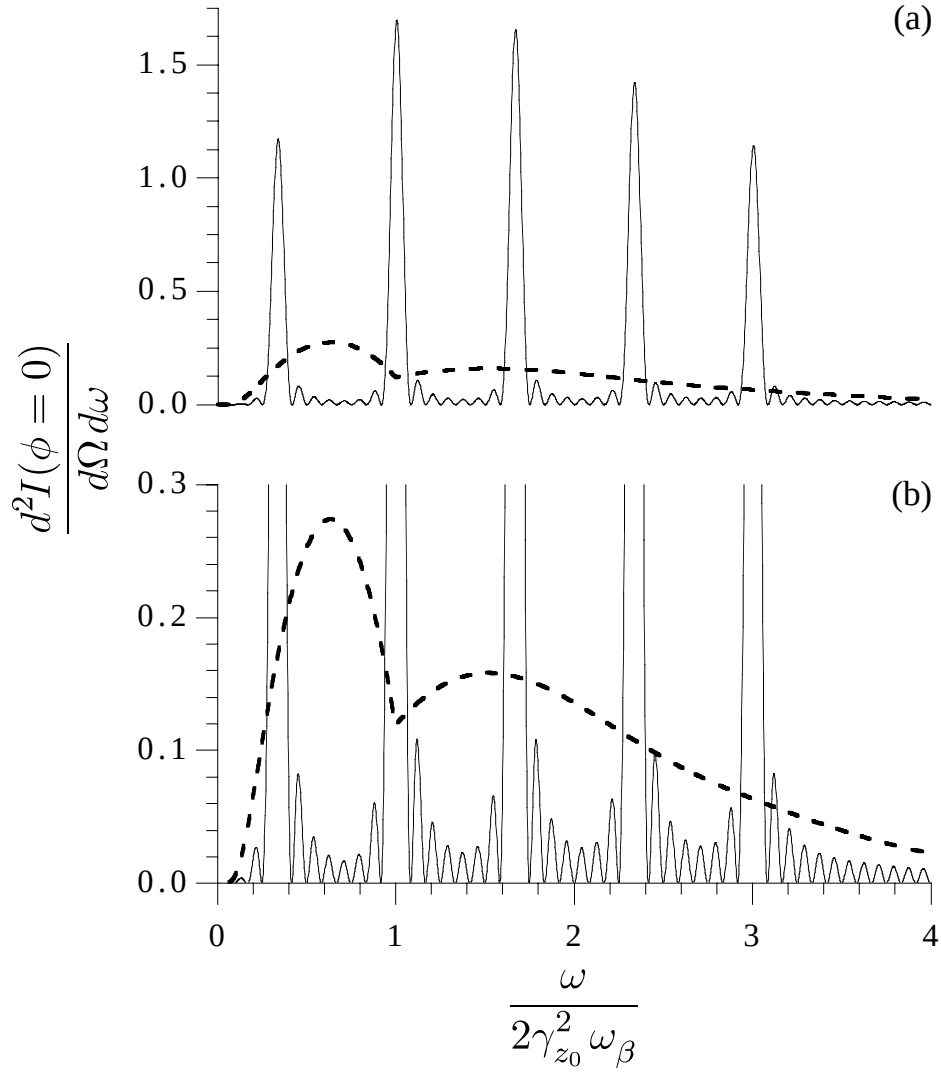

FIG. 5. Normalized spectrum $d^2I(0)/d\omega\delta\Omega$ (arbitrary units) versus $\omega/2\gamma_{z0}^2\omega_\beta$ from a single electron with $a_\beta = 2$ (solid curve), Eq. (52), and from the analytic theory of a Gaussian beam with $a_{rms} = 2$ (dashed curve), Eq. (82), for the first several odd harmonics with $N_\beta = 4$. The bottom plot is a blow-up of the top plot.

orbits is clearly to smooth out the spectrum, since the frequency of the radiation emitted by a single electron is a strong function of a_β.

In general, the integration over the beam distribution in Eq. (77) must be performed numerically. The results of such a numerical integration of Eq. (77) are shown in Figs. 6-8 for the case of an axisymmetric beam with a Gaussian radial distribution with $a_{rms} = 2$. The result for a single electron, as obtained from Eq. (42) with $N_\beta = 4$ and $a_\beta = 2$, is shown in Fig. 6, which shows the spectral density $d^2I/d\hbar\omega d\Omega$ (normalized to $\alpha_f \gamma_{z0}^2$) versus normalized frequency $\hat{k} = k/2\gamma_{z0}^2 k_\beta$ and angle $\hat{\theta} = \gamma_{z0}\theta$, for (a) $\phi = 0$ and (b) $\phi = \pi/2$. The results of averaging only over a_β (for fixed ϕ) are shown in Fig. 7, for (a) $\phi = 0$ and (b) $\phi = \pi/2$. The results of averaging over only ϕ for $a_\beta = 2$ is shown in Fig. 8(a), whereas the results of averaging over both ϕ and a_β are shown in Fig. 8(b). The effects of averaging over a_β leads to a dramatic smoothing of the radiation spectrum.

VI. ION CHANNEL LASER

Under special conditions, e.g., sufficiently high electron beam quality, self-amplified spontaneous emission (SASE) can occur whereby the incoherent synchrotron radiation emitted by the electrons is amplified via the ion channel laser (ICL) mechanism [14]. In the ICL instability, the radiation beats with the betatron motion to create an axial $\mathbf{v} \times \mathbf{B}$ (i.e., ponderomotive) force that leads to bunching of the electron beam and growth of the radiation field. This can lead to large levels of semi-coherent or coherent radiation. In SASE, the incoherent, spontaneous radiation acts as a seed for the instability, in a manner analogous to the SASE mode of operation in a free electron laser (FEL) [30].

There are important differences between the ICL and FEL mechanisms, however, that limit the SASE mode of operation. For electrons undergoing betatron motion in a plasma focusing channel, the resonant frequency of the radiation emitted along the axis is $\omega = 2\gamma_{z0}^2 n\omega_\beta/(1 + a_\beta^2/2)$, as indicated by Eq. (50). For an FEL, the resonant frequency is $\omega = 2\gamma_{z0}^2 n\omega_w/(1 + a_w^2/2)$, where $\omega_w = ck_w = 2\pi c/\lambda_w$, λ_w is the wiggler wavelength,

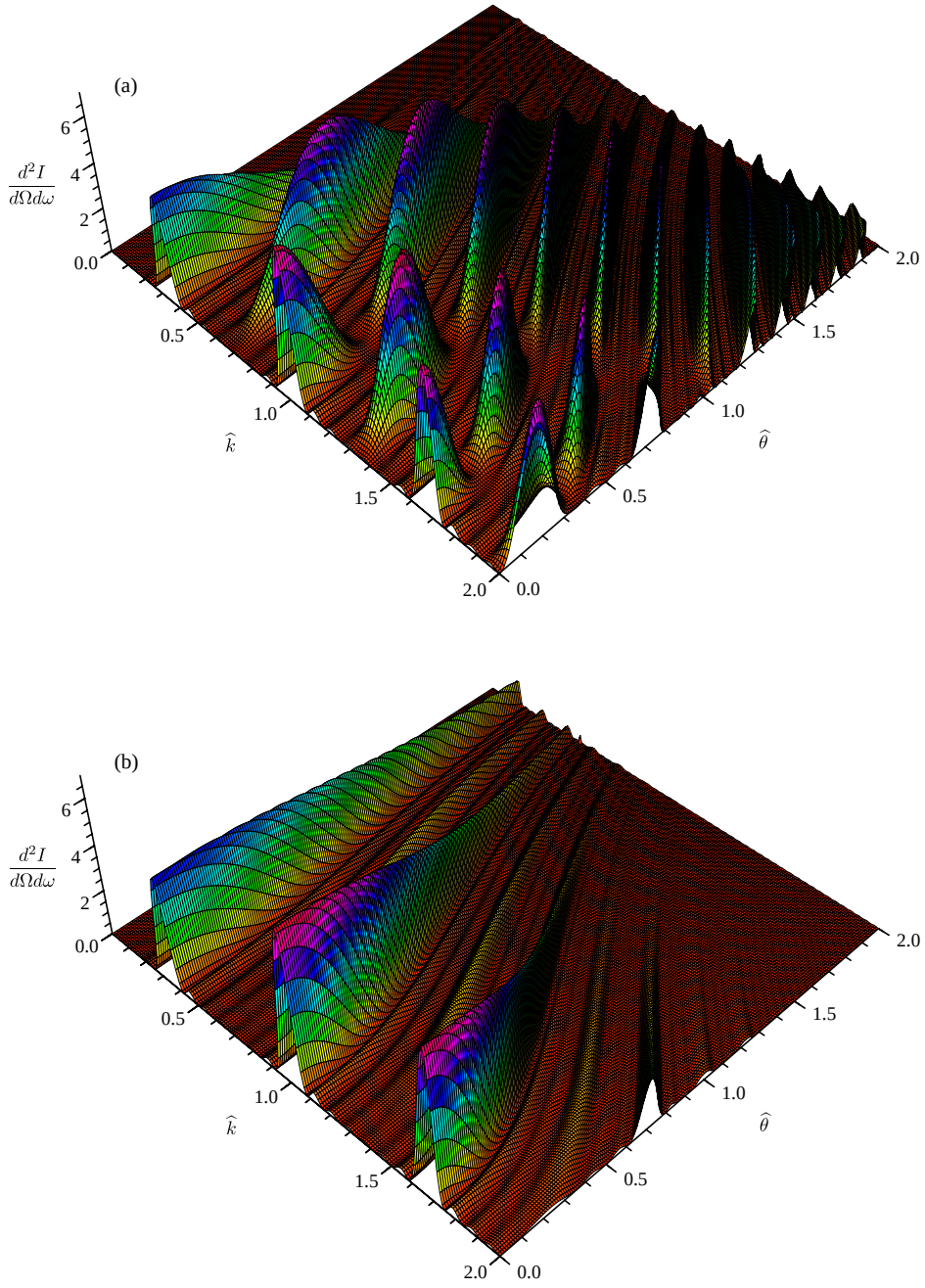

FIG. 6. Normalized spectrum $d^2I/d\omega\delta\Omega$ (arbitrary units) versus normalized frequency $\hat{k}$ and angle $\hat{\theta}$ from a single electron with $a_\beta = 2$ and $N_\beta = 4$ for (a) $\phi = 0$ and (b) $\phi = \pi/2$.

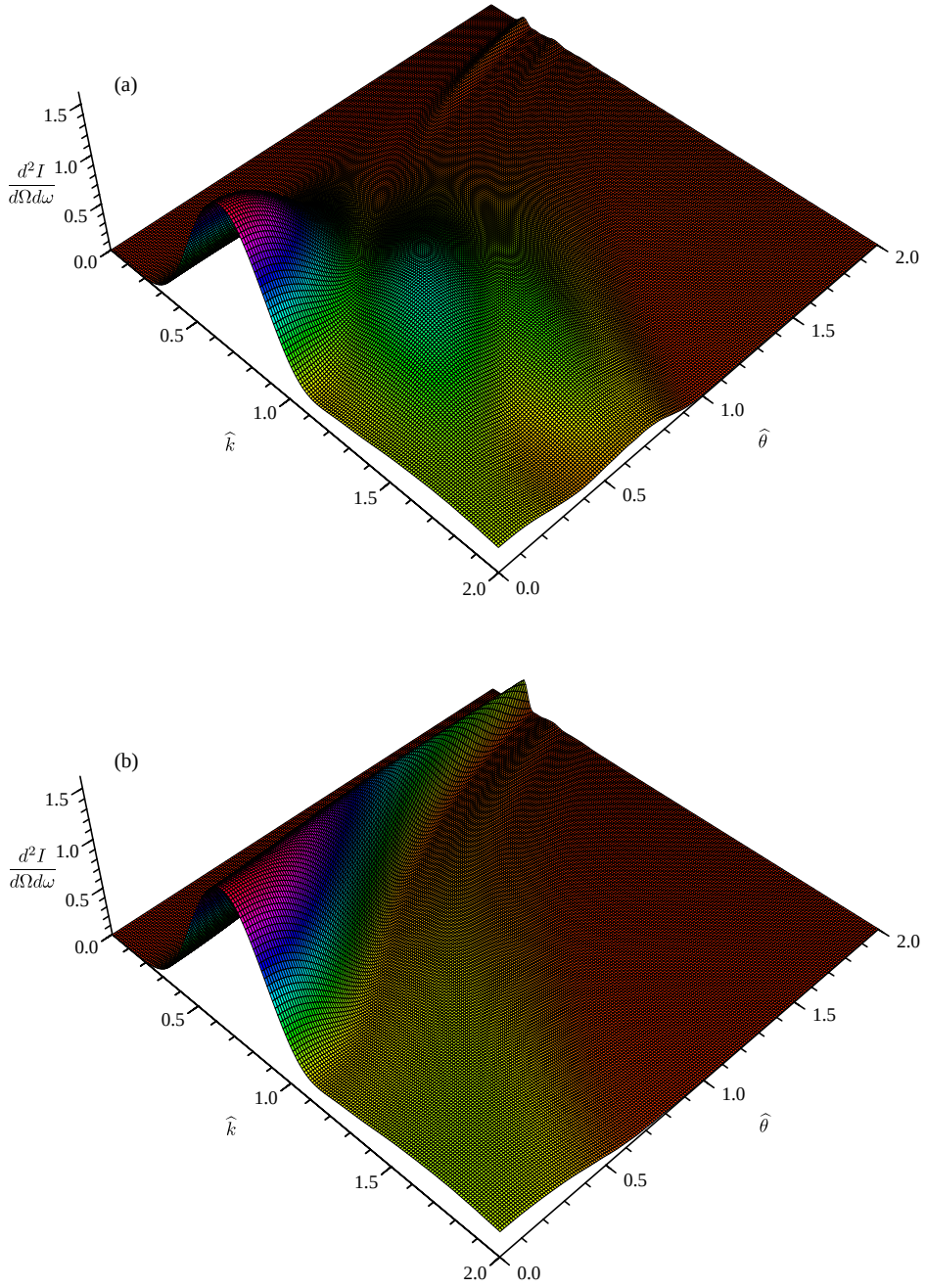

FIG. 7. Normalized spectrum $d^2I/d\omega\delta\Omega$ (arbitrary units) versus normalized frequency $\hat{k}$ and angle $\hat{\theta}$ after averaging over a Gaussian a_β distribution with $a_{rms} = 2$ and $N_\beta = 4$ for (a) $\phi = 0$ and (b) $\phi = \pi/2$.

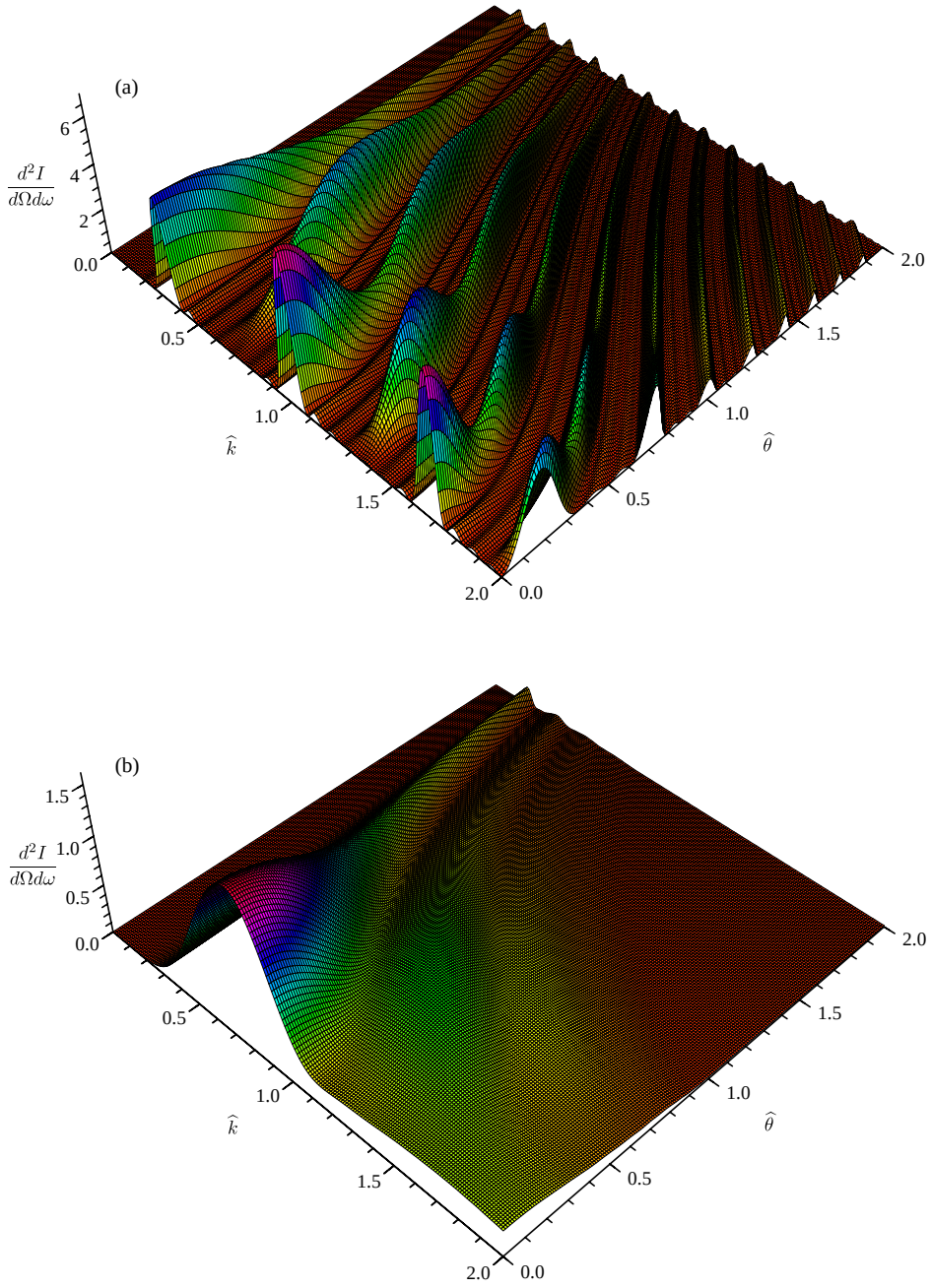

FIG. 8. Normalized spectrum $d^2I/d\omega\delta\Omega$ (arbitrary units) versus normalized frequency $\hat{k}$ and angle $\hat{\theta}$ after (a) averaging over ϕ with $a_\beta = 2$ and (b) averaging over both ϕ and a_β with $a_{rms} = 2$ and $N_\beta = 4$.

$a_w = eB_w/k_w m_e c^2$ is the wiggler strength, and B_w is the field amplitude of the wiggler magnet. In an ideal FEL, a_w is a constant since all the electrons experience the same value of B_w. This is contrast to the focusing channel, in which $a_\beta = \gamma_{z0} k_\beta r_\beta$ is a function of both the electron energy γ_{z0} and the radial position of the electrons via the betatron amplitude r_β. If a mono-energetic beam of finite radius is injected into a focusing channel (without any special tapering), electrons at different radii will have different betatron amplitudes r_β, different values of a_β, and hence different resonant frequencies.

Furthermore, for an ideal FEL with a planar wiggler of the form $\mathbf{B} = B_w \cos(k_w z)\mathbf{e}_x$, all of the beam electrons wiggle in the same plane with the same amplitude, i.e., $\mathbf{u}_\perp = a_w \cos(k_w z)\mathbf{e}_x$. Consequently, radiation emitted by all the electrons will have similar polarization. This is in contrast to the focusing channel, in which the betatron motion, and hence the synchrotron radiation, will have a variety of polarizations in the x-y plane, depending on the position and angle of the electron as it enters the channel. Hence, to amplify radiation of a given frequency and polarization in a focusing channel, only those beam electrons with the proper values of γ_{z0} and r_β will be resonant with the radiation, and only a subset of these will have the proper polarization. This is contrast to an ideal FEL, in which all the electrons in a mono-energetic beam are resonant with the radiation field with the proper polarization. This effect may be mitigated somewhat by using a drive beam with a highly elliptical cross section, such that the resulting wakefield (or blowout channel) will be highly elliptical. This could result in transverse focusing forces that are more planar and, consequently, betatron oscillations and synchrotron radiation with nearly the same polarization.

It is straightforward to quantify some of the conditions necessary for SASE to occur in a plasma focusing channel. In the following discussion, it is assumed that $k_\beta^2 r_\beta^2 \ll 1$. Consider an ideal mono-energetic electron beam of radius r_b injected into a focusing channel such that the beam centroid is along the z axis. A electron moving along the axis would have a betatron amplitude of $r_\beta = 0$, whereas an electron residing at the edge of the beam would have a betatron amplitude of $r_\beta = r_b$. For the beam to emit radiation along the axis with a

narrow bandwidth $\Delta\omega/\omega \ll 1$, it is necessary that $a_\beta^2 \ll 1$ for all the electrons. This implies that the radiation wavelength satisfy $\lambda > \pi r_b/\gamma$. For a matched beam with a normalized emittance ϵ_n, the matched-beam radius is $r_{bm} = (\epsilon_n/\gamma k_\beta)^{1/2}$, and the condition $a_\beta^2 \ll 1$ implies

$$\lambda \gg \pi\epsilon_n/\gamma. \tag{83}$$

It is interesting to note the similarity of this condition with that usually required of a SASE FEL [30], $\lambda > 4\pi\epsilon_n/\gamma$.

The condition $\Delta\omega/\omega \ll 1$, however, is not sufficient for the SASE process to occur. A more stringent condition is that the normalized axial energy spread $\Delta\gamma_z/\gamma_z$ be small compared to the so-called Pierce or gain parameter ρ, i.e., $\Delta\gamma_z/\gamma_z \ll \rho$, where by analogy with an FEL,

$$\rho = \left[\frac{a_\beta k_{pb}}{4\gamma^{3/2}k_\beta}F_\Delta^2(a_\beta)\right]^{2/3}, \tag{84}$$

where $k_{pb} = 4\pi n_b e^2/m_e c^2$, n_b is the beam density, and

$$F_\Delta(a_\beta) = J_0\left(\frac{a_\beta^2/4}{1+a_\beta^2/2}\right) - J_1\left(\frac{a_\beta^2/4}{1+a_\beta^2/2}\right). \tag{85}$$

In terms of the beam current $I_b = ec\pi n_b r_b^2$, and evaluating the expression for ρ at $r_\beta = r_b$, gives

$$\rho = \left(I_b F_\Delta^4/4\gamma I_A\right)^{1/3}, \tag{86}$$

where $I_A = m_e c^3/e = 17$ kA. Using the equations of motion for an electron in a focusing channel, Eqs. (8)-(11), the normalized energy spread is $\Delta\gamma_z/\gamma_z \simeq a_\beta^2/4$, for a beam with a centroid along the axis. Hence, $\Delta\gamma_z/\gamma_z < \rho$ implies $a_\beta^2 < 4\rho$ or $\lambda > \pi r_b/(2\gamma\rho^{1/2})$. For a matched beam, this gives

$$\lambda > \frac{\pi\epsilon_n}{4\gamma\rho}. \tag{87}$$

This is considerably more stringent that the usual FEL constraint $\lambda > 4\pi\epsilon_n/\gamma$, since typically $\rho \ll 1$. For the parameters of the E-157 experiment, $\rho \simeq 5\times 10^{-3}$.

In principle, it may be possible to tailor the energy distribution and radial profile of the beam such that a greater fraction of the beam electrons are in resonance with the radiation

field. For example, consider a mono-energetic, very narrow beam of width Δr_b injected off-axis such that the centroid of the beam executes betatron oscillations of amplitude $r_\beta = r_{b0}$ with $r_{b0} \gg \Delta r_b$ [40]. In this case, all of the electrons in the beam would undergo approximately the same betatron orbit and would have approximately the same value for a_β, i.e., the spread in a_β is given by $\Delta a_\beta/a_\beta \simeq \Delta r_b/r_{b0}$. In this case the condition $\Delta\omega/\omega \ll 1$ implies $\Delta r_b/r_{b0} \ll (1 + a_\beta^2/2)/a_\beta^2$, which in principle, could be easily satisfied. The more stringent condition, $\Delta\gamma_z/\gamma_z < \rho$, implies $\Delta r_b/r_{b0} < 2\rho/a_\beta^2$, which could be satisfied for sufficiently small values of a_β.

Even if the condition $\Delta\gamma_z/\gamma_z < \rho$ is satisfied, it is not clear that the SASE process would occur. In a conventional FEL, SASE requires that a number of conditions be satisfied (in addition to $\Delta\gamma_z/\gamma_z < \rho$) [30], i.e., $\epsilon_n < \gamma\lambda/4\pi$, $N_\beta\lambda_\beta \gg L_G$, $L_G < L_R$, and $N_\beta\lambda < L_e$, where N_β is the number of betatron oscillations, $L_G \simeq 0.046\lambda_\beta/\rho$ is the gain length, $L_R = \pi w_0^2/\lambda$ is the Rayleigh length of the radiation with spot size w_0, and L_e is the electron bunch length. Furthermore, for the case of an ICL driven by a narrow beam with a centroid undergoing betatron oscillations, it is likely that the gain (i.e., ρ) is reduced since the geometric overlap between the electron beam and the radiation is reduced, due to the betatron motion of the centroid. Such novel ICL configurations require a detailed analysis.

VII. SUMMARY

Spontaneous radiation emitted from an electron undergoing betatron motion in a plasma focusing channel was analyzed starting from basic principles. Application of these results to the E-157 experiment and to the ICL were examined. Important similarities and differences between SASE in an FEL and in an ICL were delineated. In particular, the spontaneous radiation emitted along the axis of a plasma focusing channel from a single electron occurs near the resonant frequency $\omega_n = 2\gamma_{z0}^2 n\omega_\beta/(1 + a_\beta^2/2)^{1/2}$. The role of the betatron strength parameter a_β is analogous to that of the wiggler strength parameter a_w (or K_w) in FEL physics. In Ref. [14], the ICL was considered only in the limit $a_\beta^2 \ll 1$. When $a_\beta^2 \ll 1$,

radiation is emitted primarily at the fundamental frequency $\omega = 2\gamma_{z0}^2\omega_\beta$ and is independent of a_β. For $a_\beta \gtrsim 1$, however, the resonant frequency is a strong function of a_β and radiation is emitted in numerous harmonics extending out to the critical harmonic number $n_c = 3a_\beta^3/4$. This is the case in the E-157 experiments, in which $a_\beta \sim 2 - 50$.

In an ideal FEL, the wiggler strength parameter a_w is a constant (a function of only the magnetic field of the wiggler) for all of the beam electrons. However, in an ICL, $a_\beta = \gamma_{z0}k_\beta r_\beta$ depends on both the electron energy γ_{z0} and the betatron amplitude r_β. Since r_β, and hence a_β, is different for every electron in a typical beam, this places serious limits on the possibility of realizing a SASE ICL. For an electron beam with a centroid along the z-axis, a radius r_b and $a_\beta(r_b) > 1$, the radiation from the beam is no longer emitted at discrete harmonics as it would be from a single electron with $r_\beta = r_b$. Rather, since $0 < a_\beta \lesssim a_\beta(r_b)$ for the electrons in the beam, the resulting radiation is in the form of a broad continuum as indicated by Figs. 5 - 8, even for the case of an initially mono-energetic beam. In the limit $a_\beta^2 \ll 1$, the radiation from the beam could be nearly monochromatic at the fundamental frequency. The condition $a_\beta^2 \ll 1$ implies $\lambda \gg \pi\epsilon_n/\gamma$ for a matched beam, which is similar to the criterion $\lambda > 4\pi\epsilon_n/\gamma$ often quoted for a SASE FEL. The condition $a_\beta^2 \ll 1$, however, is not sufficient to insure that the SASE ICL process will occur. A more stringent condition for the occurrence of SASE is on the axial energy spread of the beam within the focusing channel, i.e., $\Delta\gamma_z/\gamma_z \ll \rho$, where ρ is the effective Pierce (or gain) parameter. Again, since r_β varies across the beam, there exists a large energy spread $\Delta\gamma_z/\gamma_z \simeq a_\beta^2/4$. The condition $\Delta\gamma_z/\gamma_z \ll \rho$ implies $\lambda > \pi\epsilon_n/(4\gamma\rho)$ for a matched beam. Since typically $\rho \ll 1$, this restriction on the radiated wavelength $\lambda > \pi\epsilon_n/(4\gamma\rho)$ is much more stringent than that in a conventional SASE FEL. Furthermore, the betatron orbits in a typical beam in a focusing channel are not polarized in the same plane as they are in a conventional FEL. This also can reduce the gain in a SASE ICL. These arguments, however, assumed an untailored electron beam centered about the channel axis. It may be possible to relax this constraint on the radiated wavelength in a SASE ICL by appropriately tailoring the electron beam, for example, a narrow electron beam injected off-axis such that all of the beam electrons execute approximately the same betatron

orbit. Such novel ICL configurations require further analysis to assess their viability.

VIII. ACKNOWLEDGMENTS

The authors acknowledge useful conversations with the participants of the Working Group on Plasma Wakefield Accelerators at the Advanced Accelerator Concepts Workshop (Santa Fe, NM, June 200) and with the members of the E-157 collaboration. This work was supported by the Department of Energy under contract No. DE-AC-03-76SF0098.

REFERENCES

[1] For a review see, E. Esarey et al., IEEE Trans. Plasma Sci. **24**, 252 (1996).

[2] R. Govil, W. P. Leemans, E. Yu. Backhaus, and J.S. Wurtele, Phys. Rev. Lett. **83**, 3202 (1999).

[3] N. Barov, J B. Rosenzweig, M.E. Conde, W. Gai, and J.G. Power, Phys. Rev. ST Accel. Beams **3**, 011301 (2000)

[4] J. Ng et al., SLAC Preprint, SLAC-PUB-8501 (2000); SLAC E-150 web site, URL http://www.slac.stanford.edu/exp/e150.

[5] M.J. Hogan et al., Phys. Plasmas **7**, 2241(2000); SLAC E-157 web site, URL http://www.slac.stanford.edu/grp/arb/e157.

[6] K. Takayama and S. Hiramatsu, Phys. Rev. A **37**, 173 (1988).

[7] W.A. Barletta and A.M. Sessler, in *High Gain, High Power Free Electron Laser: Physics and Application to TeV Particle Acceleration* edited by R. Bonifacio, L. De Salvo Souza and C. Pellegrini (North-Holland, Amsterdam, 1989) p. 211-20.

[8] L.H. Yu, A.M. Sessler, and D.H. Whittum, Nucl. Instrum. Methods A **318**, 721 (1992).

[9] D.H. Whittum, S. Hiramatsu, and J.S. Kim, IEEE Trans. Plasma Sci. **21**, 170 (1993).

[10] K. Takayama et al., J. Appl. Phys. **77**, 5467 (1995).

[11] C. Joshi, T. Katsouleas, J.M. Dawson, Y.T. Yan, and J. Slater, IEEE J. Quantum Electron. **23**, 1571 (1987).

[12] R.L. Williams, C.E. Clayton, C. Joshi, and T.C. Katsouleas, IEEE Tran. Plasma Sci. **21**, 156 (1993).

[13] K.R. Chen and J.M. Dawson, Phys. Rev. Lett. **68**, 29 (1992); Phys. Rev. A **45**, 4077 (1992).

[14] D.H. Whittum, A.M. Sessler, and J.M. Dawson, Phys. Rev. Lett. **64**, 2511 (1990); D.H. Whittum, Phys. Fluids B **4**, 730 (1992).

[15] J.B. Rosenzweig et al., Phys. Rev. A **44**, 6189 (1991).

[16] W.E. Martin, G.J. Caporaso, W.M. Fawley, D. Prosnitz, and A.G. Cole, Phys. Rev. Lett. **54**, 685 (1985).

[17] H.L. Buchanan, Phys. Fluids **30**, 221 (1987).

[18] J. Krall, K. Nguyen, and G. Joyce, Phys. Fluids B **1**, 2099 (1989).

[19] S.B. Swanekamp, J.P. Holloway, T. Kammash, and R.M. Gilgenbach, Phys. Fluids B **4**, 1332 (1992).

[20] D.H. Whittum , W.M. Sharp, S.S. Yu, M. Lampe, and G. Joyce, Phys. Rev. Lett. **67**, 991 (1991).

[21] M. Lampe, G. Joyce, and D. H. Whittum, Phys. Fluids B 5, 1888 (1993).

[22] J. Krall and G. Joyce, Phys. Plasmas **2**, 1326 (1995).

[23] A.A. Geraci and D.H. Whittum, Phys. Plasmas **7**, 3431 (2000).

[24] P. Catravas et al., Proc. 1999 Particle Accelerator Conf., Ed. by A. Luccio and W. Mackay (IEEE, Piscataway NJ, 1999), pp. 2111-2113.

[25] P. Catravas et al., Phys. Rev. E **64**, 046502, (2001).

[26] C.E. Clayton et al., "Dynamic focusing and envelope oscillations of a 28.5 GeV electron beam in a long plasma," submitted to Phys. Rev. Lett. (2001).

[27] W.A. Barletta et al., Nuc. Instr. Meth. A **423**, 256 (1999).

[28] E. Esarey, P. Catravas, and W.P. Leemans, in *Advanced Accelerator Concepts*, edited by P. Colestock and S. Kelly, AIP Conf. Proc. **569** (Amer. Inst. Phys., NY, 2001), pp. 473-486.

[29] S. Wang et al., "Observation of spontaneous emitted X-ray betatron radiation in beam-plasma interactions", Proc. 2001 Particle Accelerator Conf., to be published.

[30] *Handbook of Accelerator Physics and Engineering*, edited by A.W. Chao and M. Tigner (World Scientific, Singapore, 1999).

[31] S. Wang and C. Joshi, private communication.

[32] D.H. Whittum et al., IEEE Trans. Plasma Sci. **21**, 136 (1993).

[33] M. Reiser, *Theory and Design of Charged Particle Beams* (Wiley, New York, 1994).

[34] J.D. Jackson, *Classical Electrodynamics*, 2nd ed. (Wiley, New York, 1975), Chap. 14.

[35] T. Katsouleas, private communication.

[36] E. Esarey, S.K. Ride, and P. Sprangle, Phys. Rev. E **48**, 3003 (1993).

[37] S.K. Ride, E. Esarey and M. Baine, Phys. Rev. E **52**, 5425-5442 (1995).

[38] H. Wiedemann, *Particle Accelerator Physics II* (Springer-Verlag, New York, 1995).

[39] *Handbook of Mathematical Functions*, edited by M. Abramowitz and I.A. Stegun (Dover, New York, 1972), p. 369.

[40] In collaboration with the working group on plasma wakefield accelerators, Advanced Accelerator Concepts Workshop, Santa Fe, NM, June (2000).